www.lajss.org
Latin American Journal of Solids and Structures 2 (2005) 167–193

Material influence on the response of impacted beams

Marcílio Alves[a,*] and J.L. Yu[b]

[a]Department of Mechatronics and Mechanical Systems Engineering
University of São Paulo – São Paulo – SP – 05508-900 – Brazil
[b]Department of Modern Mechanics, University of Science and Technology of China – Hefei – China

Abstract

The dynamic response of elastic-plastic beams is studied numerically using several material constitutive models which take into account material strain hardening and strain-rate hardening. A comparison is drawn between the beam responses of these more sophisticated models and the ones predicted by a rigid, perfectly plastic material law. A method for choosing the material parameters in the bilinear model is proposed. The numerical simulation shows the importance of the elastic effect which reduces the plastic work absorption as well as causes part of the plastic work to be dissipated during vibration. The study reported here allows a better understanding of the influence of various material parameters on the dynamic response of structures and helps to establish some limits of validity for the rigid, perfectly plastic analysis.

1 Introduction

Over the past few decades, the phenomenon of impact in structures has been investigated in detail [8]. While the initial motivation in the 60's and 70's was mainly for the development of military technology, interest in the field has now spread to the civil area [9], with applications ranging from automotive structures [16, 18] to environmental disasters [14].

The inelastic response of structures under large impact loads has found important applications in the design of transportation systems [7]. Passenger cars, containers transporting hazardous substances, nuclear casks, pipes in chemical plants, oil rigs and many other structures have now to be crashworthy in order to comply with safety codes issued by governments and institutional bodies.

The most common approach for basic analysis of impacted structures assumes that the material is rigid-perfectly plastic (RPP), ie a material with no elastic deformation and a constant flow stress, regardless of the strain level. In fact, the so-called rigid-perfectly plastic analysis, established in the 50's, was upgraded to impact analysis by taking into account inertia forces in the equilibrium equations and strain rate effects on the flow stress.

*Corresponding author E-mail: maralves@usp.br Received 23 May 2005; In revised form 17 June 2005

Within some limitations, it is possible to use numerical schemes to perform complex analysis of real structures under impact loading [3,5]. However, the details yielded by these analyses are in some cases less important than some global parameters, for example, maximum permanent displacement and the associated impact energy. Moreover, despite the fact that supercomputers are capable of dealing with very complicated structures using a wide variety of material models, rigid-perfectly plastic simplification is still used for metal structures, especially in dynamic cases. Hence, for a large-scale structure or in a preliminary design stage, a rough estimation of structural response by a simplified model is of practical significance.

Nonetheless, hardly any material behaves as perfectly plastic, which poses an important question, namely, the accuracy of perfectly plastic analysis when dealing with materials exhibiting important strain hardening and strain rate effects.

It has been found that, for some materials such as mild steel, copper, lead and titanium alloys, the yield stress as well as the post-yield flow stress increase with the strain rate. Various viscoplastic constitutive models were proposed and applied to describe the phenomenon of material strain-rate sensitivity and recent progress in this area can be found in Reference [12].

Obviously, theoretical analyses become more complicated even for a very simple structure when strain-rate sensitivity of material is taken into account since the strain rate in a structure varies with position and time. To overcome this difficulty, some simplifications were introduced in the analysis of structural impact. Symonds [21], for instance, suggested an approximate viscous relation to simplify the analysis, later modifyed in Reference [1].

Within the framework of the rigid-perfectly plastic theory, the strain rate effect of materials on the structural response is introduced by a characteristic strain rate. Hence, the quasi-static flow stress is replaced by a dynamic value estimated under that strain rate [8, 17]. In some cases, good agreement is obtained between simplified method of analysis and experimental data. However, it is obvious that the error caused by such simplifications alone is uncertain and the general method for choosing a characteristic strain-rate remains unsolved.

Strain hardening is another effect which cannot be considered in the rigid-perfectly plastic model. When this effect is significant, the error is not negligible if the initial yield stress is used in the model since most impact phenomena involve large strains. Experimental results show that in such cases a better agreement with the RPP prediction can be obtained if another value for the flow stress, e.g. the ultimate tensile stress (UTS), is considered [11, 17, 20, 22].

Elastic effects of the material on the structure response to dynamic loads have been studied by many authors [6, 19, 23, 27]. The results show the importance of elastic wave propagation during the early stage of response of simple structures, like beams.

Although numerical simulations using Finite Element (FE) Methods are widely used in structural analysis, less work has been done on the comparison of numerical results with those yielded by the rigid-perfectly plastic methods applied to elemental structures. This is an important issue because the RPP methods are widely used to predict several features of the response of an impacted structure due to its simplicity and easy of use.

It should be emphasised that small changes in the material strain hardening or strain rate

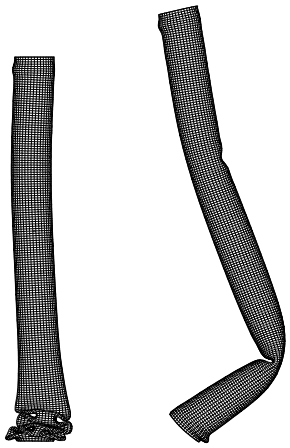

(a) 9.0m/s (b) 9.0m/s

Figure 1: Buckling transition for a tube with $L = 630$ mm and made from material with low sensitivity to the strain rate. (a) no strain rate effect is considered. (b) strain rate effect is taken into account. The labels indicate the impact velocity.

response can substantially affect the strucuture response. Accordingly, it is important to have at hand a rational way to choose the flow stress, as here endeavoured. To give an example of the importance of using an accurate flow stress if errors are to be avoided, consider the axial impact of the aluminium tube investigated in Reference [10]. There, the material response is such that the flow stress changes by only 6% for a strain rate of $\dot{\varepsilon} = 15/s$, i.e. a low strain rate sensitive material. Even so, for this range of strain rates, two very distinct structural responses are obtained if strain rate effects are or not considered, Figure 1. In this case, a tube having length $L = 630$ mm collapses progressively, when assuming a strain-rate insensitive material, but responds by a global bending mode to the same impact velocity when strain-rate effects are taken into account.

The importance of chosing a proper flow stress is explored here by comparing the response of beams subjected to dynamic loads as given by a FE analysis using different material models with those yielded by the RPP methods. By so doing, it is possible to investigate how the strain and strain rate hardening influence the beam response. Moreover, one can propose a correction for the flow stress used to represent the material behaviour in the RPP analysis to improve the comparison with FE results based on a experimental material description.

2 Material and structure models

The non-linear relationship between the flow stress and strain for most metals makes difficult an analytical treatment of a structural problem envolving large strains. Clearly, to model a material using a single flow stress makes the analysis more tractable, although fine details of the response cannot be predicted.

A bilinear material offers a better description of the material behaviour, possibly offering a balance between simplicity and exactness. Hence, it is important to compare the exact response of a structure with that predicted by a model which adopts either a perfectly plastic or a bilinear material.

Numerical tests are performed to simulate the response of aluminium alloy and mild steel beams under various dynamic loadings. It is known that, unlike mild steel, aluminium alloy is not a strain-rate sensitive material. In order to examine the effect of material properties on the response, different material models are used and comparisons are made to reveal the importance of the material property or to find a practical approach to obtain a simplified model.

The basic idea is that the difference in the response of a beam modelled with real material properties and that modelled with a simplified material model under the same dynamic loading could be attributed mainly to the simplification of the material behaviour. Obviously, the error yielded by any simplification depends on the range of the response of interest. Here, it is focused on medium finite deformations, ie when the final deflection is one to three times of the beam height.

2.1 Structure description

Two kinds of beams, namely cantilevers and fully clamped beams, were investigated. The dimensions of the cantilever beams were $H = 10$mm, $B = 8$mm and $L = 100$mm. For a fully clamped beam, the cross-section is kept the same, only the length is changed to $L = 200$mm.

These beams were analysed numerically using the finite-element code ABAQUS [4]. It is assumed that the numerical response provided by the code when using experimental material properties is comparable to the experimental structural response to a very good degree [24, 26].

Two dimensional, 8-node, biquadratic, isoparametric, plane stress finite elements with reduced integration were used to model the cantilever and clamped beam, Figure 2. A total of 356 and 404 elements were used for the cantilever and fully clamped beams, respectively. In order to reduce the effect of stress concentration at the support, the meshing of the beams was extended 32 mm inwards the clamped boundary, Figure 2. The elements in this region were fully restrained at the lower and end surfaces.

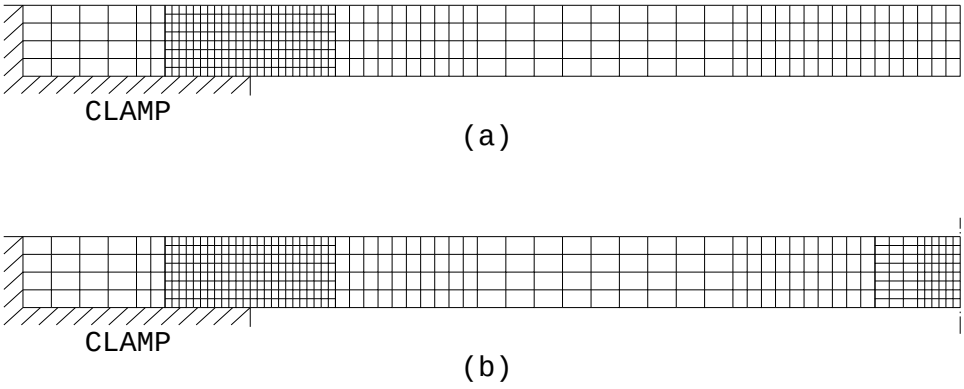

Figure 2: Mesh for the (a) cantilever and (b) clamped beam.

2.2 Loading description

Three basic types of dynamic load were applied to the beams. The first one is the impact of a mass at the centre of the clamped beam and at the tip of the cantilever. The case of a uniformly distributed load throughout the beam span for both beams was also considered. The last case analysed was that of a concentrated load applied at the centre of the clamped beam and at the tip of the cantilever. The pulse loads have the characteristics indicated in Figure 3, whereas the load and beam types used in this investigation are summarised in Figure 4. The values for impact mass, impact velocity, pulse duration and pulse intensity were changed as indicated in Section 3.

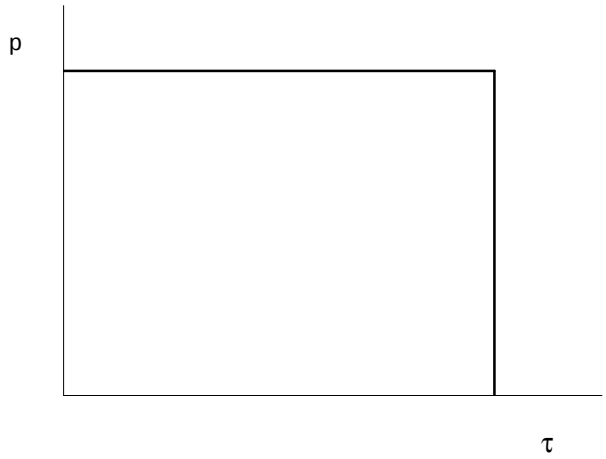

Figure 3: Rectangular pulse load used in this investigation. The actual pulse intensity, p, and its duration, τ, are indicated in Section 3.

In the case of an impact mass, a mass element was used and it was assumed that the mass

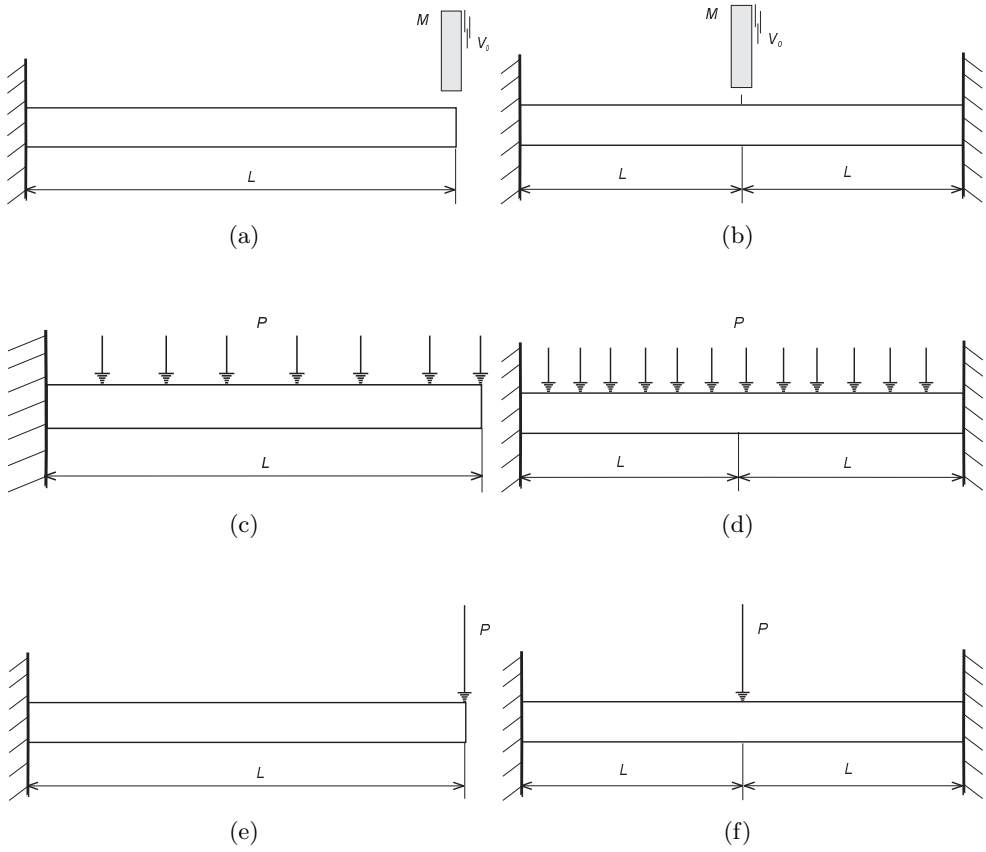

Figure 4: Beam configuration used in this investigation. (a) and (b) Cantilever and clamped beam under an impact mass, respectively. (c) and (d) Cantilever and clamped beam under a distributed dynamic load, respectively. (e) and (f) Cantilever and clamped beam under a concentrated dynamic load, respectively.

Material	ρ (kg/m3)	E (GPa)	ν	σ_y (MPa)	σ_u (MPa)	σ_f (MPa)	ε_u^p	ε_f^p	D (1/s)	p
Aluminium alloy	2,700	72.0	0.300	115.0	351.0	440.0	0.153	0.520	—	—
Mild steel	7,800	208.0	0.286	259.0	546.0	784.0	0.176	0.830	1.05e7	8.3

Table 1: Main mechanical material properties of the two materials used in the numerical simulation [25].

remains in full contact with the beam throughout the response. The contact area in this case is assumed to be finite, 2 mm and 4 mm along the axial direction for cantilevers and clamped beams, respectively. This was arrived at by reducing the degree in the transverse direction of the associated nodes, i.e., all nodes in the contact area have the same displacement in the transverse direction. Similar constraints are applied to the case of a concentrated load.

2.3 Material modelling

Two materials were used as a reference in this study; a mild steel, known to be strain rate sensitive, and an aluminium alloy whose main mechanical properties are not strain rate sensitive. They were experimentally characterised both static and dynamically in Reference [25] and Table 1 lists their main properties. The quasi-static equivalent stress–strain curve for the aluminium and mild steel are depicted in Figure 5.

By adopting in the numerical simulation the equivalent stress–strain curves shown in Figure 5 one arrives at what is here considered the exact solution for the impact response of the beams. Alternatively, the numerical simulation can be run using simplified constitutive laws, ie

- Elastic, linear plastic (bi-linear) material without rate-sensitivity.
- Rigid, linear plastic material without rate-sensitivity.
- Rigid, perfectly plastic material without rate-sensitivity.
- Elastic, linear plastic (bi-linear) material with rate-sensitivity, catered by a characteristic strain rate.

These constitutive laws are represented in Figure 6. It is evident by comparing Figures 5 and 6 that a major issue to be investigated is which value of the elastic modulus, flow stress and strain rate should be used in the simplified material models in order to represent consistently the real material behaviour.

It seems reasonable to retain the real values of the stress and the plastic strain at failure. In order to select a value for the yield stress in a bilinear elastic-plastic model, numerical simulations are conducted using material properties of aluminium alloy. Two possible material constants

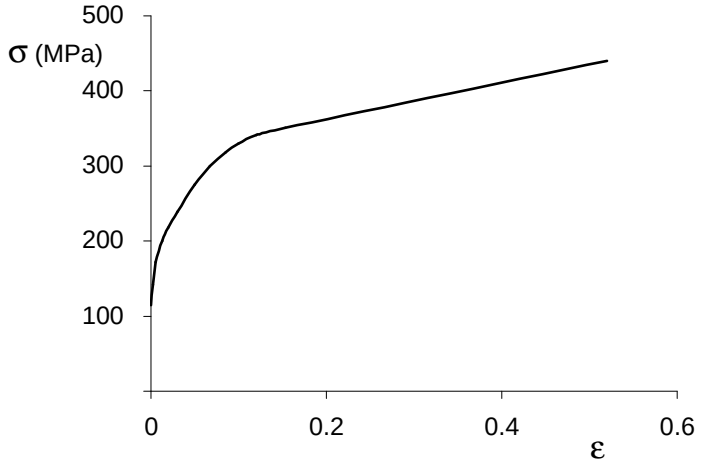

(a)

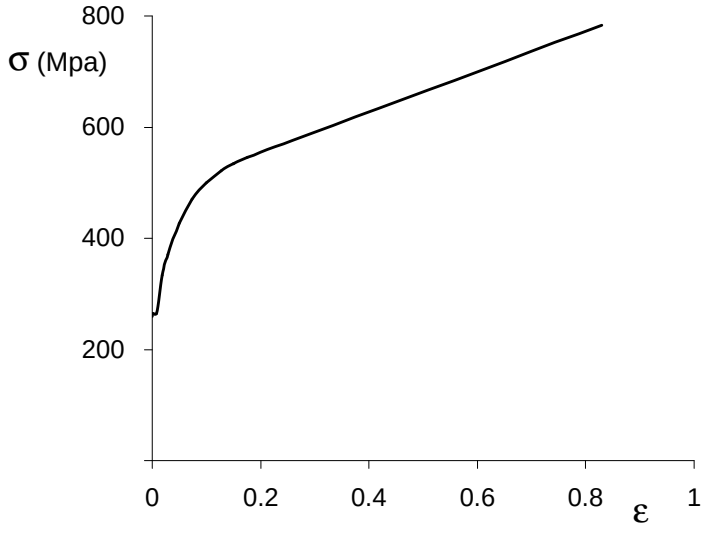

(b)

Figure 5: Quasi-static equivalent stress-strain curve for (a) aluminium and (b) mild steel.

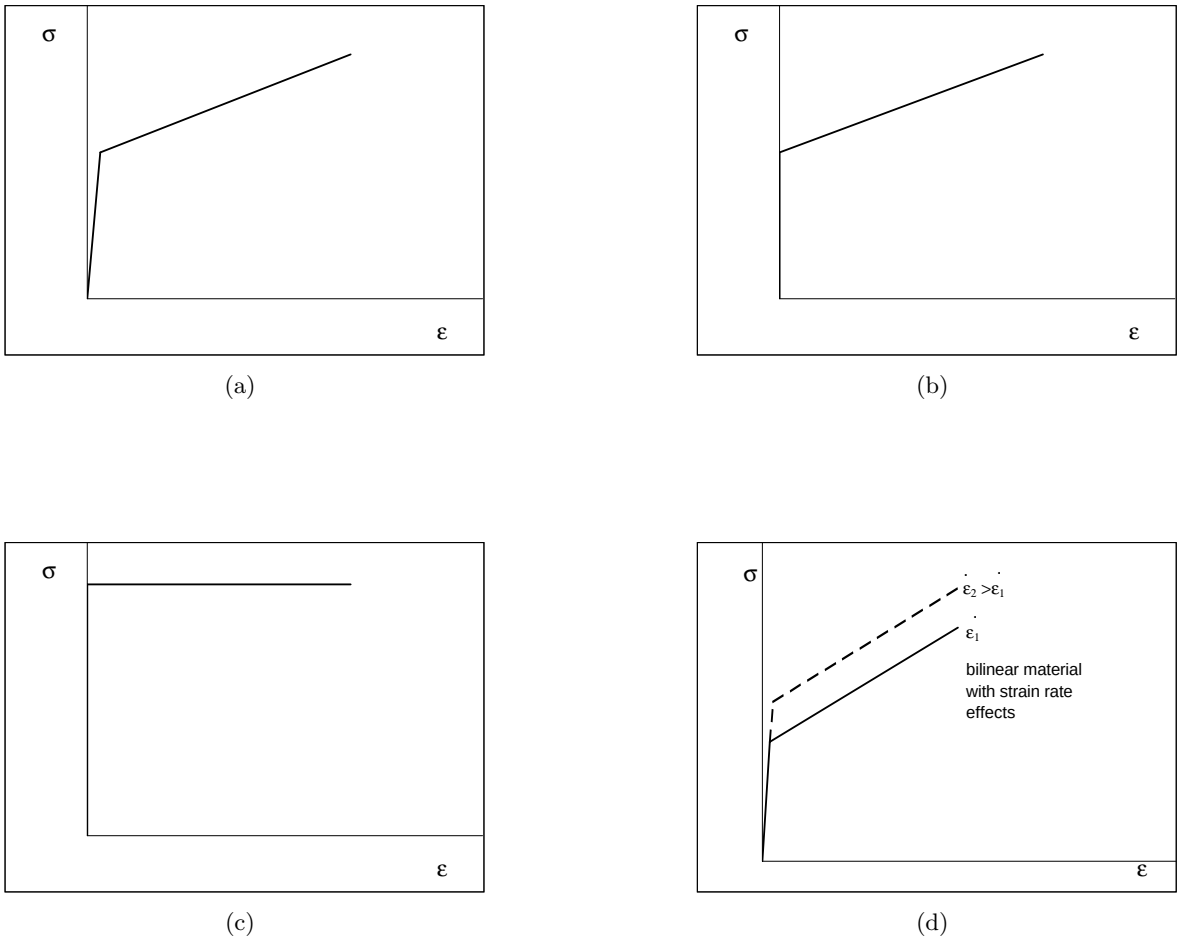

Figure 6: Material models used in the simulation. (a) Elastic, linear plastic (bi-linear) without rate-sensitivity, (b) Rigid, linear plastic material without rate-sensitivity, (c) Rigid, perfectly plastic material without rate-sensitivity, (d) Elastic, linear plastic (bi-linear) with rate-sensitivity.

could be used. One is the true yield stress, σ_y, and the other is extrapolated from the values of stress and plastic strain at failure, σ_f and ε_f^p, respectively, and those at the point of ultimate tensile strength, σ_m and ε_m^p, to the point with zero plastic strain,

$$\sigma_1 = \frac{\sigma_m \varepsilon_f^p - \sigma_f \varepsilon_m^p}{\varepsilon_f^p - \varepsilon_m^p}. \tag{1}$$

However, using the actual yield stress as the flow stress for the bilinear model, one will underestimate the material resistance to plastic deformation. Conversely, using equation 1 one will overestimate it. Thus, it is explored here the use of an intermediate value for the flow stress, σ_n, such that

$$\sigma_n = \sigma_y + \frac{\sigma_1 - \sigma_y}{n}. \tag{2}$$

In the present work, three different values for n are considered, namely $n = 2$, $n = 3$ and $n = 4$.

For a structure made from a strain-rate hardening material, as the mild steel described by Table 1, the stress distribution depends not only on the strain field but also on the velocity gradient field. In order to simplify the strain-rate hardening behaviour, it is a common practice to introduce a characteristic strain rate and then replace the real constitutive equation by a rate-independent stress-strain relation associated with the characteristic strain rate. This simple approach has provided good agreement with experiments since a significant change of flow stress will take place only when the order of magnitude of strain rate changes.

One of the most popular equations to cater for strain rate effects on the flow stress is due to Cowper and Symonds [8] and can be written as

$$\sigma_{0_d} = \sigma_{0_s} \left[1 + \left(\frac{\bar{\dot{\varepsilon}}}{D} \right)^{1/p} \right], \tag{3}$$

where σ_{0_d} and σ_{0_s} are the dynamic and static flow stress, respectively; $\bar{\dot{\varepsilon}}$ is the average strain rate and D and p are material constants whose value for the mild steel used here are listed on Table 1.

One can now define a strain rate factor

$$\alpha = 1 + \left(\frac{\bar{\dot{\varepsilon}}}{D} \right)^{1/p} \tag{4}$$

such that the yield, ultimate and failure stresses used in equations (1) and (2) can now be multiplied by α. This, in turn, provides a correction for the material strain rate sensitivity and allows the strain rate effects to be taken into account when using a bilinear stress–strain curve.

The key factor to reach a reasonable result for the estimation of the strain rate hardening is to estimate the characteristic strain rate.

For a cantilever, plastic deformation occurs mainly near the support for all load cases studied here. So the strain and strain rate distributions are spatially non-uniform and the average strain-rate can be estimated by

$$\bar{\dot{\varepsilon}} = \frac{W_m}{4kT\sqrt{L^2 - W_m^2}} \tag{5}$$

where W_m is the maximum deflection and T is the associated time. Although the maximum deflection, W_m, and the response time, T, are not known a priori, a rough estimate is possible. In considering the fact that the flow stress changes significantly only when the order of magnitude of the strain rate changes, such estimate is enough for engineering practice. However, in order to make comparisons, W_m and T are calculated from the numerical results using true material data, with the difference between the total strain and the plastic strain being neglected.

In equation (5), k is the dimensionless length of the plastic region with respect to the beam height. Various suggestions for the bending hinge length exist within the framework of the rigid-perfectly plastic model [15]. According to Mosquera et al. [13], values of $k = 2$ and (roughly) $k = 3$ can be arrived at by considering the ratio of the dynamic to static plastic bending moment. Additionally, a value of $k = 3.333$ was also selected based on the work of Alves and Jones [2], who suggested a length of the plastic region equal to one third of the beam length for a cantilver with a rectangular cross section.

For a fully clamped beam, membrane deformation becomes dominant when the transverse deflection exceeds the beam height. Thus, the average axial strain, $\bar{\varepsilon}_m$, from the transverse deflection is given approximately by

$$\bar{\varepsilon}_m = \sqrt{1 + \left(\frac{W_m}{L}\right)^2} - 1, \tag{6}$$

yielding an average strain rate of

$$\bar{\dot{\varepsilon}}_m = \frac{\sqrt{1 + \left(\frac{W_m}{L}\right)^2} - 1}{T}. \tag{7}$$

This method is used to simulate the responses of fully clamped mild steel beams under different dynamic loads. The static yield stress in this model is calculated using equation (2) with $n = 3$ due to reasons to be discussed later.

Lastly, elastic effects on the dynamic response of the beams were explored by comparing numerical results which used real material, rigid-linear plastic and rigid-perfectly plastic material models. Unfortunately, as the ABAQUS code does not provide any rigid-plastic model, a Young's modulus as high as 100 times the actual value was used to represent a rigid material model.

2.4 Rigid-perfectly plastic prediction

Numerical simulations and analytical calculations are performed to find the value of yield stress in the rigid-perfectly plastic model which will predict nearly the same final deflection as that

calculated by the true material model.

The theoretical response for various beam configurations and load types based on rigid, perfectly plastic methods are grouped as follows [8]:

- Cantilever under a concentrated load

$$\frac{W_f}{H} = \frac{6\tau^2 P}{\rho B H^2}\left(\frac{1}{\sigma_y B H^2} - \frac{1}{4LP}\right) \qquad \text{when} \quad \eta \leq 3 \tag{8}$$

$$\frac{W_f}{H} = \frac{4\tau^2 P^2}{\rho \sigma_y B^2 H^4}\left(1 + \frac{2\ln(\eta/3)}{3}\right) \qquad \text{when} \quad \eta > 3 \tag{9}$$

- Cantilever under a distributed load

$$\frac{W_f}{H} = \frac{3\tau^2 p}{4\rho H^2}\left(\frac{2pL^2}{\sigma_y H^2} - 1\right) \tag{10}$$

where

$$\eta = \frac{4LP}{\sigma_y B H^2} \tag{11}$$

- Fully clamped beam under distributed load

$$\frac{W_f}{H} = \frac{\sqrt{1 + 2\eta(\eta-1)(1-\cos(\gamma\tau))} - 1}{2} \qquad \text{when} \quad \gamma\tau \leq \pi \tag{12}$$

where

$$\eta = \frac{pL^2}{\sigma_y H^2} \qquad \gamma = \sqrt{\frac{3\sigma_y}{\rho L^2}} \tag{13}$$

- Fully clamped beam under a central mass impact

$$\frac{W_f}{H} = \frac{\sqrt{1 + \frac{LV_0^2\left(2M + \frac{4\rho BHL}{3}\right)}{\sigma_y B H^3}} - 1}{2} \tag{14}$$

Test Number	P (kN)	τ (ms)	Material model	T (ms)	W_m (mm)	W_f (mm)	Error (%)
1	1.6	0.125	Real	0.694	13.28	9.67	
			Bilinear $n = 2$	0.629	10.83	7.12	-26.4
			Bilinear $n = 3$	0.662	11.92	8.73	-9.7
			Bilinear $n = 4$	0.690	12.66	9.80	1.3
			Rigid-Linear	0.529	6.47	6.44	-33.4
2	1.6	0.200	Real	0.905	24.62	20.37	
			Bilinear $n = 2$	0.818	20.07	16.32	-19.9
			Bilinear $n = 3$	0.943	23.18	19.54	-4.1
			Bilinear $n = 4$	1.000	25.23	21.73	6.7
			Rigid-Linear	0.812	15.74	15.70	-22.9

Table 2: Results for aluminium cantilever under a concentrated load.

3 Results

3.1 Aluminium beams

For cantilever aluminium beams under a concentrated load, one load magnitude of 1.6 kN and two pulse durations of $\tau = 0.125$ms and $\tau = 0.200$ms were used. The response of the aluminium cantilever to these loads are such that the final displacement varies roughly between H and $2H$.

It was noted that, due to the material elasticity, the cantilever reaches a maximum displacement, W_m, at time T and springs back, reaching a final displacement, W_f, after several oscilations.

Table 2 lists the main results for the two loading conditions when using four different material models, ie bilinear with $n = 2$, $n = 3$ and $n = 4$, and rigid-linear plastic [1].

The response given by the numerical simulation is compared to the one also obtained numerically but now using the actual equivalent stress–strain curve. The error due to the material law simplification is also listed on the Table.

Similarly, Table 3 list the same variables as in the previous case but now for a cantilever loaded uniformly throughout its span. The load intensities chosen are now $p = 6.0$MPa, $p = 9.0$MPa and $p = 12.0$MPa, applied during $\tau = 0.1$ms.

The case of a distributed load applied uniformly along the fully clamped beam is listed on Table 4. In this case, the loads are $p = 10.0$MPa and $p = 20.0$MPa, again acting during the same interval $\tau = 0.1$ms.

[1] For aluminium, $\sigma_y = 115$ MPa, $\sigma_1 = 314$ MPa, $\sigma_f = 440$ MPa, $\varepsilon_f^p = 0.52$, so $\sigma_2 = 214.5$ MPa, $E_{h_2} = 433.7$ MPa, $\sigma_3 = 181.3$ MPa, $E_{h_3} = 497.5$ MPa, $\sigma_4 = 164.8$ MPa, $E_{h_4} = 529.3MPa$, for $n = 2$, $n = 3$ and $n = 4$, respectively.

Test Number	p (MPa)	τ (ms)	Material model	T (ms)	W_m (mm)	W_f (mm)	Error (%)
1	6.0	0.10	Real	0.707	12.16	8.92	
			Bilinear $n = 2$	0.545	10.07	6.85	-23.2
			Bilinear $n = 3$	0.717	11.29	8.28	-7.2
			Bilinear $n = 4$	0.750	12.17	9.08	1.8
			Rigid-Linear	0.731	8.62	8.60	-3.6
2	9.0	0.10	Real	0.843	22.51	18.17	
			Bilinear $n = 2$	0.801	20.41	15.85	-12.8
			Bilinear $n = 3$	0.887	23.10	19.40	6.8
			Bilinear $n = 4$	0.962	24.77	21.40	17.8
			Rigid-Linear	0.842	19.61	19.57	7.7
3	12.0	0.10	Real	0.983	34.41	29.68	
			Bilinear $n = 2$	1.000	33.73	29.48	-0.7
			Bilinear $n = 3$	1.117	37.96	34.12	15.0
			Bilinear $n = 4$	1.183	40.44	36.86	24.2
			Rigid-Linear	1.055	34.05	34.01	14.6

Table 3: Results for aluminium cantilever under a distributed load.

Test Number	p (MPa)	τ (ms)	Material model	T (ms)	W_m (mm)	W_f (mm)	Error (%)
1	10.0	0.10	Real	0.433	10.79	9.00	
			Bilinear $n = 2$	0.417	9.99	7.89	-12.3
			Bilinear $n = 3$	0.437	10.87	9.07	0.8
			Bilinear $n = 4$	0.456	11.37	9.71	7.9
			Rigid-Linear	0.471	8.72	8.70	-3.3
2	20.0	0.10	Real	0.392	21.47	20.31	
			Bilinear $n = 2$	0.399	20.77	19.26	-5.2
			Bilinear $n = 3$	0.422	22.44	21.20	4.4
			Bilinear $n = 4$	0.440	23.43	22.37	10.1
			Rigid-Linear	0.436	20.99	20.97	3.2

Table 4: Results for a fully clamped aluminium beam under a distributed load.

Test Number	M (kg)	V_0 (m/s)	Material model	T (ms)	W_m (mm)	W_f (mm)	Error (%)
1	2.00	5.00	Real	3.929	12.10	10.17	
			Bilinear $n = 2$	3.878	11.45	9.25	-9.0
			Bilinear $n = 3$	4.158	12.37	10.40	2.3
			Bilinear $n = 4$	4.278	12.90	11.03	8.5
			Rigid-Linear	4.514	11.26	11.24	10.5
2	6.00	5.00	Real	6.528	21.17	19.45	
			Bilinear $n = 2$	6.580	20.73	18.62	-4.3
			Bilinear $n = 3$	7.015	22.13	20.48	5.3
			Bilinear $n = 4$	7.324	23.00	21.55	10.8
			Rigid-Linear	6.911	21.36	21.34	9.7

Table 5: Results for a fully clamped aluminium beam under a mass impact.

Table 5 refers to the case of a fully clamped aluminium beam under an impact mass $M = 2$kg and $M = 6$kg hitting the beam with a velocity $V_0 = 5$m/s.

3.2 Mild steel

For the mild steel beams, it is necessary to take into account strain rate effects on the material response. In order to explore this phenomenon, the simulations were processed using bilinear material models with a fixed $n = 3$ in equation (2) but different estimations of the average strain rate. Three values for α in equation (4) were used. They are associated with three different plastic zone sizes, ie hinge lengths of $2H$, $3H$ and $3.33H$. Also, a rigid-linear material model was investigated with $n = 3$ and a hinge length of $3.33H$. The results for displacement were compared with the ones obtained using the actual mild steel equivalent stress–strain curve.

Table 6 is related to a cantilever under a concentrated load of $P = 3.20$kN applied during $\tau = 0.15$ms, $\tau = 0.20$ms and $\tau = 0.30$ms. In Table 7, the results refer to the cantilever subjected to a distributed load $p = 20$MPa and $p = 30$MPa, when $\tau = 0.10$ms. For this same pulse duration, Table 8 refers to the case of a fully clamped beam under the various distributed loads indicated in the table. Finally, Table 9 presents results for a fully clamped mild steel beam under the central impact of a mass.

4 Discussion

The rigid, perfectly plastic methods of analysis has been successfuly used in the analysis of many types of basic structures, operating both under static and dynamic loads. The major material

Test Number	P (kN)	τ (ms)	Material model	T (ms)	W_m (mm)	W_f (mm)	α	Error (%)
			Real	0.810	11.44	9.18		
			Bilinear $n = 3$	0.700	10.01	7.74	1.202	-15.7
1	3.20	0.15	Bilinear $n = 3$	0.703	10.07	7.84	1.192	-14.6
			Bilinear $n = 3$	0.707	10.08	7.87	1.190	-14.3
			Rigid-Linear	0.593	5.66	5.64	1.190	-38.6
			Real	0.974	17.32	14.81		
			Bilinear $n = 3$	0.944	14.98	12.57	1.208	-15.1
2	3.20	0.20	Bilinear $n = 3$	0.947	15.10	12.68	1.198	-14.4
			Bilinear $n = 3$	0.949	15.12	12.71	1.195	-14.2
			Rigid-Linear	0.769	9.73	9.70	1.195	-34.5
			Real	1.232	31.31	28.51		
			Bilinear $n = 3$	1.232	27.88	25.06	1.218	-12.1
3	3.20	0.30	Bilinear $n = 3$	1.248	28.13	25.35	1.207	-11.1
			Bilinear $n = 3$	1.248	28.19	25.42	1.205	-10.8
			Rigid-Linear	1.092	20.76	20.74	1.205	-27.3

Table 6: Results for a mild steel cantilever under a concentrated load.

Test Number	p (MPa)	τ (ms)	Material model	T (ms)	W_m (mm)	W_f (mm)	α	Error (%)
			Real	1.000	19.76	17.09		
			Bilinear $n = 3$	0.921	18.23	15.69	1.210	-8.2
1	20.0	0.10	Bilinear $n = 3$	0.930	18.36	15.84	1.200	-7.3
			Bilinear $n = 3$	0.932	18.39	15.90	1.198	-7.0
			Rigid-linear	0.878	15.88	15.86	1.198	-7.2
			Real	1.233	36.62	33.58		
			Bilinear $n = 3$	1.287	37.33	34.51	1.222	2.8
2	30.0	0.10	Bilinear $n = 3$	1.306	37.59	34.81	1.212	3.7
			Bilinear $n = 3$	1.312	37.66	34.88	1.209	3.9
			Rigid-linear	1.250	34.75	34.72	1.209	3.4

Table 7: Results for a mild steel cantilever under a distributed load.

Test Number	p (MPa)	τ (ms)	Material model	T (ms)	W_m (mm)	W_f (mm)	α	Error (%)
1	25.0	0.10	Real	0.510	11.05	9.85		
			Bilinear $n = 3$	0.496	10.72	9.32	1.192	-5.4
			Rigid-linear	0.460	8.91	8.89	1.192	-9.7
2	40.0	0.10	Real	0.493	17.93	17.06		
			Bilinear $n = 3$	0.500	17.52	16.42	1.218	-3.8
			Rigid-linear	0.494	16.17	16.16	1.218	-5.3
3	80.0	0.10	Real	0.443	35.64	34.93		
			Bilinear $n = 3$	0.485	37.24	36.63	1.257	4.9
			Rigid-linear	0.493	36.43	36.42	1.257	4.3

Table 8: Results for a fully clamped mild steel beam under a distributed load.

Test Number	M (kg)	V_0 (m/s)	Material model	T (ms)	W_m (mm)	W_f (mm)	α	Error (%)
1	4.0	5.00	Real	3.975	12.10	10.86		
			Bilinear $n = 3$	4.004	11.86	10.40	1.152	-4.2
			Rigid-linear	3.898	11.08	11.06	1.152	1.8
2	10.0	5.00	Real	6.232	19.74	18.73		
			Bilinear $n = 3$	6.313	19.68	18.31	1.164	-2.2
			Rigid-linear	6.228	19.10	19.09	1.164	1.9
3	10.0	7.00	Real	6.216	27.44	26.50		
			Bilinear $n = 3$	6.330	27.91	26.90	1.177	1.5
			Rigid-linear	6.337	27.46	27.44	1.177	3.5

Table 9: Results for a fully clamped mild steel beam under a mass impact.

parameter underlying such analysis is the flow stress, which is sometimes taken as the material yield stress, the ultimate stress or even the fracture stress. The choice of which value is to be used depends on whether or not a more conservative design is sought or whether the ultimate capacity of the structure to bear loads is aimed, or even if a better correlation with experimental data is in play.

In fact, the present study clearly shows that the flow stress is not an easy parameter to choose in order to predict correctly the final displacement of cantilevers and clamped beams. Moreover, it is obvious that real materials exhibit strain and strain rate herdening, which become significant for large values of load acting over short time. Hence, it is important to access how a better representation of the use of a bilinear material model improves the response description.

Inspection of equation (2) shows that large values of n make the flow stress in a bilinear model approach the material yield stress. It is believed that the range of $n \in [2, 4]$ is reasonable and the results for different cases when $n = 2$, $n = 3$ and $n = 4$ are summarised in Tables 2 to 5.

Generally speaking, when the intensity of load and consequently the transverse deflection are small, a small value of the yield stress, or, a lager n should be chosen. However, it appears that the relative error depends not only on the magnitude of the loading and the value of n, but also on the *type* of structure. For example, a better result is achieved for an aluminium cantilever if $n = 4$ and $W/H \sim 1$. If $W/H \sim 2$, then $n = 3$ gives better results and if $W/H \sim 3$ a good choice is $n = 2$.

For fully clamped aluminium beams, $n = 3$ and $n = 2$ lead to a better result for $W/H \sim 1$ and $W/H \sim 2$, respectively, regardless of the load being distributed or concentrated.

Nevertheless, it seems that when $n = 3$, the errors caused by a bilinear simplification are acceptable for most cases studied here. This value for n is used to model the mild steel, allowing to focus the investigation on the strain rate effects.

The results for mild steel cantilevers under different dynamic loads are listed in Tables 6 and 7. Here the value of α instead of k is shown, the largest value of α corresponding to the smallest value of k ($k = 2.0$). It appears that all results for strain rate sensitive cantilevers under concentrated loads underestimate the final deflection, though $k = 3.333$ gives relatively better results. On the other hand, for cantilevers under distributed loads, the error strongly depends on the intensity of the dynamic load.

For fully clamped mild steel beams under distributed load and impacted by a mass, the results in Tables 8 and 9 indicate a good agreement for the final displacement at the beam centre when using a real material and a bilinear and rigid-linear material, with $n = 3$.

Using equations (8) to (14), it is possible to calculate the final displacement of cantilevers under a concentrated and distributed load, and of fully clamped beams under a distributed load and under an impact of a mass, respectively. Hence, it is possible to use a flow stress, σ_0^T, such that the theoretical displacement value matchs the one obtained numerically when using the real material data for the constitutive law. It is also possible to adjust the flow stress used in a numerical analysis, σ_0^N, for these cantilevers and beams when adopting a perfectly plastic

material model.

A comparison of the yield stresses required for rigid-perfectly plastic model, both numerical and theoretical, to reach the same final deflection as that calculated using true material data is listed in Tables 10 and 11.

Table 10: Flow stress required by the rigid, perfectly plastic model, to match the exact numerical final displacement of cantilevers.

Material	Load Type [a]	Test Number	W_f (mm)	σ_0^N (MPa)[b]	σ_0^T (MPa)[c]
Aluminium	C	1	9.67	137.5	137.9
		2	20.37	155.6	157.3
	D	1	8.92	184.6	188.9
		2	18.17	211.5	217.7
Mild steel	C	1	9.18	282.9	285.1
		3	28.51	331.1	337.9
	D	1	17.09	393.0	404.6
		3	33.58	458.1	474.6

[a] C: concentrated load; D: distributed load.

[b] Theoretical value of yield stress.

[c] Numerical value of yield stress.

Table 11: Flow stress required by the rigid, perfectly plastic model, to match the exact numerical final displacement of fully clamped beams.

Material	Load Type[a]	Test Number	W_f (mm)	σ_0^N (MPa)[b]	σ_0^T (MPa)[c]
Aluminium	D	1	9.00	187.0	138.2
		2	20.31	235.0	163.2
	M	1	10.17	232.3	153.4
		2	19.45	281.7	164.1
Mild steel	D	1	9.85	367.0	271.7
		2	17.06	420.7	304.9
	M	1	10.86	423.4	278.8
		2	18.73	494.0	291.6

[a] M: mass impact; D: distributed load.

[b] Theoretical value of yield stress.

[c] Numerical value of yield stress.

It is evident that a good agreement between theoretical and numerical values of the flow stress is found for cantilevers. The theoretical value is a little bit lower than the numerical one and the difference is less than 4%. However, the yield stresses obtained by numerical simulations for fully clamped beams are significantly lower than the corresponding theoretical ones.

It transpires from the deformed configurations that necking occur at the mid-span and at the supports for fully clamped beams, when a rigid-perfectly plastic model is used. No such evidence is found when the true material model is used, as shown in Figure 7. This explains the difference between the numerical and theoretical results mentioned above, since the theoretical model does not take the geometrical non-linearity of the cross-section into account.

It is obvious from Tables 10 and 11 that the yield stress required to reach the right results depends on the intensity of the load. As expected, a larger value of yield stress should be used for a stronger load. This means that the error is sensitive to the choice of the yield stress. More seriously, different values of the yield stress should be chosen for different types of loads. Figure 8(a) and (b) shows the dependence of the yield stress on the final deflection for aluminium and steel beams, respectively. It can be seen that, for the same final deflection, the yield stress for cantilevers subjected to concentrated load is higher than all other cases. Thus, a unique value suitable for all cases is impossible.

In order to explore such sensitivity, besides the value which will predict right result, two additional values of the yield stress are used, which are ± 10% different from the values listed in Tables 10 and 11. The errors of the resulted final deflection are listed in Tables 12 and 13. It is clear that cantilevers are more sensitive to the choice of yield stress than fully clamped beams.

Material	Load Type[a]	W_f[b] (mm)	Theoretical				Numerical			
			W_f^- (mm)	Error (%)	W_f^+ (mm)	Error (%)	W_f^- (mm)	Error (%)	W_f^+ (mm)	Error (%)
Aluminium	C	9.67	11.26	16.4	8.40	-13.1	11.18	15.6	8.48	-12.3
		20.37	23.81	16.9	17.65	-13.4	23.60	15.9	17.78	-12.7
	D	8.92	10.10	13.2	7.96	-10.8	10.07	12.9	7.98	-10.5
		18.17	20.47	12.7	16.29	-10.3	20.41	12.3	16.31	-10.2
Mild steel	C	9.18	10.70	16.6	7.97	-13.2	10.63	15.8	8.04	-12.4
		28.51	33.38	17.1	24.65	-13.5	33.04	15.9	24.86	-12.8
	D	17.09	19.20	12.3	15.36	-10.1	19.18	12.2	15.38	-10.0
		33.58	37.64	12.1	30.27	-9.9	37.61	12.0	30.28	-9.8

[a] C: concentrated load; D: distributed load.
[b] W_f^-: Final deflection when the yield stress is 10% lower than the required value.
W_f^+: Final deflection when the yield stress is 10% larger than the required value.

Table 12: Influence of the yield stress variation used in the rigid, perfectly plastic model, on the final deflection of cantilevers.

The numerical simulation also reveals that when material elasticity is considered, the plastic deformation will not end after the maximum deflection is reached. A typical curve of the deflection history and the corresponding energy history are shown in Figures 9 and 10, respectively.

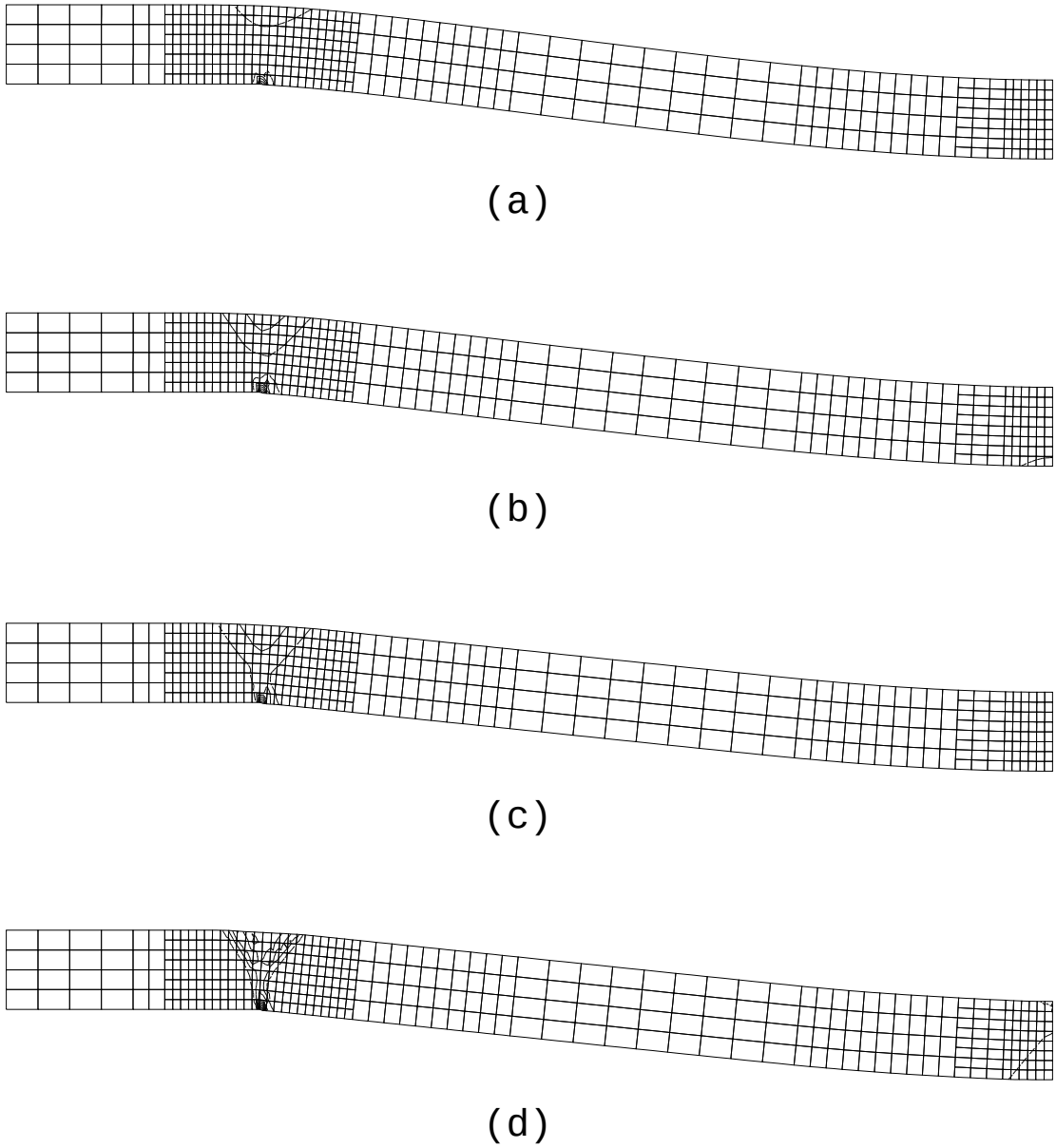

Figure 7: Distribution of the final equivalent plastic strain for a fully clamped aluminium beam under a dynamic distributed load of $p = 10$ MPa and $\tau = 0.1$ ms. The material models used are (a) true material data; (b) bilinear model; (c) rigid-linear plastic model; (d) rigid-perfectly plastic model.

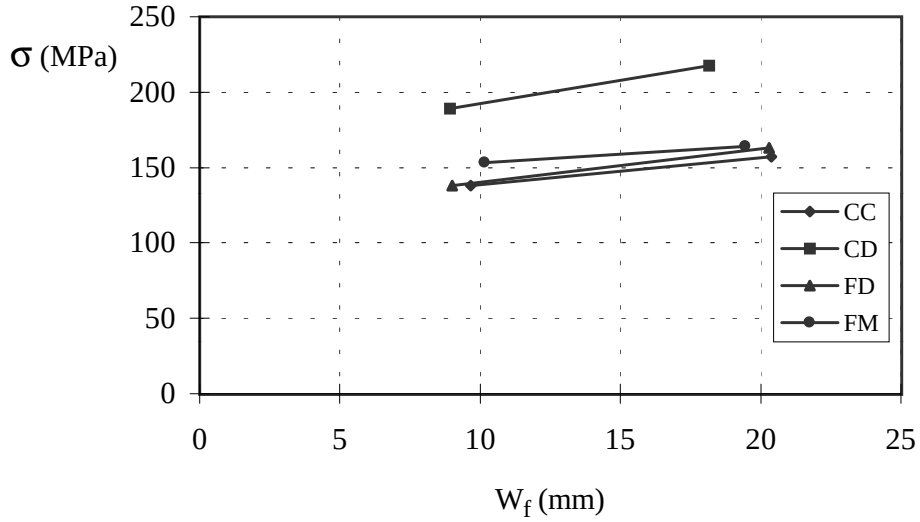

(a)

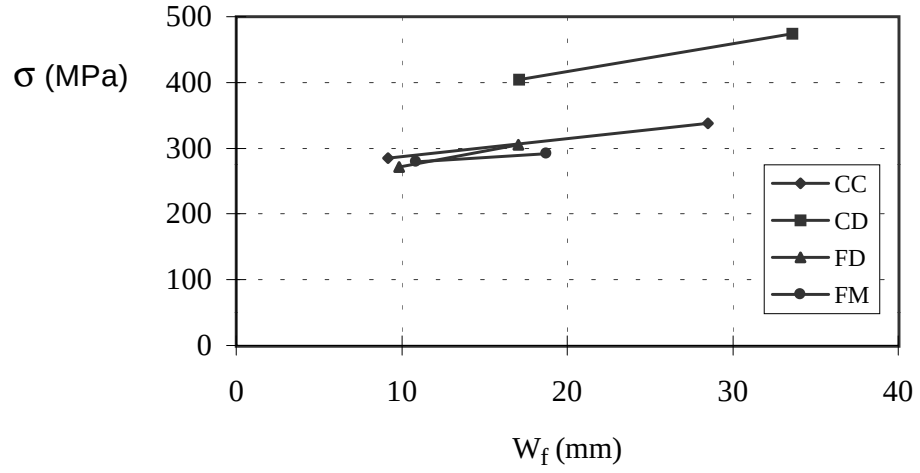

(b)

Figure 8: Flow stresses (obtained numerically when using a rigid, perfectly plastic material model) necessary to match the final deflection value with the one obtained using a real material, for different beam and load configurations. (a) aluminium alloy beams, (b) mild steel beams. CC and CD– cantilever under a concentrated and distributed load, FD and FM– fully clamped beam under a distributed load and central impact mass, respectively.

Material	Load Type	W_f (mm)	Theoretical				Numerical			
			W_f^- (mm)	Error (%)	W_f^+ (mm)	Error (%)	W_f^- (mm)	Error (%)	W_f^+ (mm)	Error (%)
Aluminium	D	9	9.78	8.70	8.33	-7.40	9.76	8.40	8.30	-7.80
		20.31	21.77	7.20	19.06	-6.20	22.54	11.00	18.57	-8.60
	M	10.17	10.91	7.30	9.54	-6.20	10.97	7.90	9.49	-6.70
		19.45	20.72	6.50	18.36	-5.60	21.07	8.30	18.13	-6.80
Mild steel	D	9.85	10.65	8.10	9.15	-7.10	10.61	7.70	9.17	-6.90
		17.06	18.29	7.20	15.99	-6.30	18.56	8.80	15.82	-7.30
	M	10.86	11.63	7.10	10.20	-6.10	11.71	7.80	10.14	-6.60
		18.73	19.96	6.60	17.67	-5.70	20.26	8.20	17.46	-6.80

Table 13: Influence of the yield stress variation used in the rigid, perfectly plastic model, on the final deflection of fully clamped beams.

M (kg)	40	10	2	0.4	0.025
V_0 (m/s)	2.5	5	11.18	25	100
W_f (mm)	18.86	18.73	18.47	17.72	12.26

Table 14: Final deflection of a fully clamped mild steel beam under a central mass impact for various values of impact velocity and mass and a fixed initial impact energy of 125J.

Due to further plastic dissipation, the amplitude of the elastic vibration decreases. It should be noticed that part of the plastic work is dissipated during unloading and reloading of the material. This feature is not considered when the rigid-perfectly plastic model is used, where all plastic work is assumed to increase the transverse deflection.

When finite deformations are considered, an assumption is often introduced to simplify the analyses in the rigid-perfectly plastic model, namely that the deformation mode is the same as in static cases and energy balance is used to obtain an analytical solution. When this method is used to cases of mass impact, this simplification implies that the final deformation depends only on the total initial kinetic energy, regardless whether a light mass or a heavy mass is used.

To explore the influence of impact velocity on the response of a fully clamped mild steel beam under a mass impact, numerical simulations are performed using real material data and maintaining the same kinetic energy. The results are shown in Table 14. Although only slight difference is found when the initial velocity is in the range of 2.0-40 m/s, care should be taken when the impact velocity is very high.

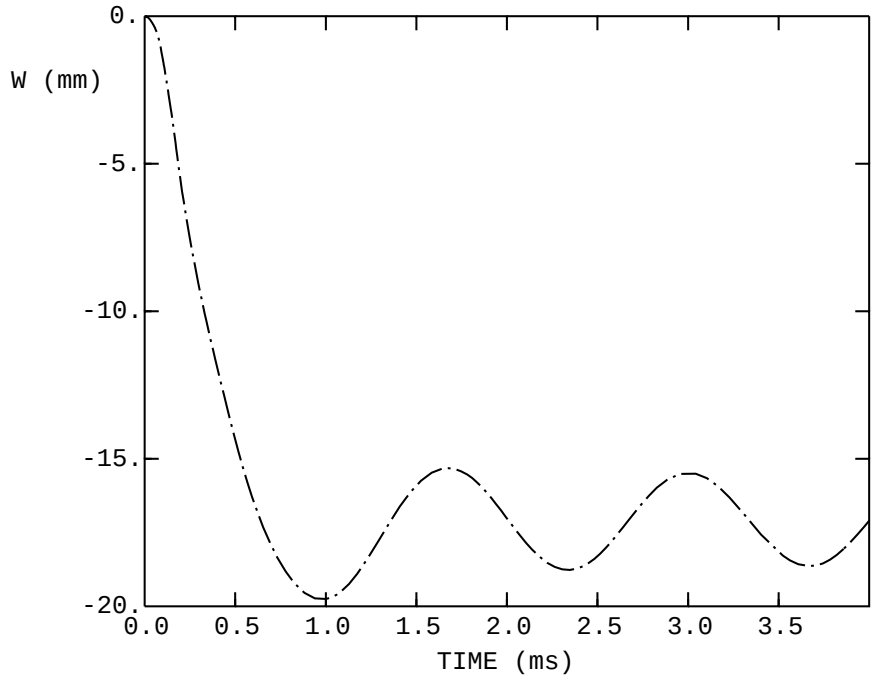

Figure 9: History of the transverse deflection at the free end of a mild steel cantilever under distributed dynamic load of p=20 MPa and τ=0.1 ms.

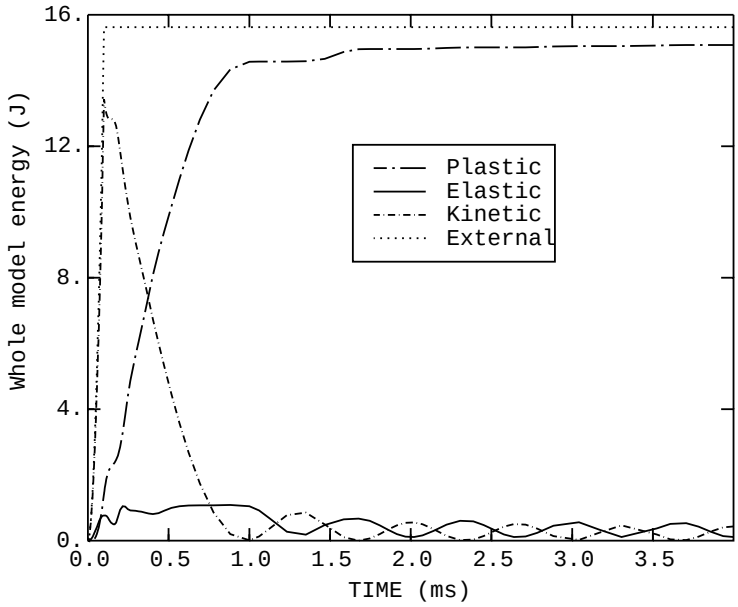

Figure 10: Variation of external work and plastic, elastic and kinetic energy with time for a mild steel cantilever under distributed dynamic load of p=20 MPa and τ=0.1 ms.

5 Conclusion

The influence of the flow stress on response of some basic beam configuration was examined in this investigation. It is evident that care should be taken in order to select a value of flow stress which is capable of predicting within a small error the final displacement of the beams analysed.

It was also shown that the flow stress used in perfectly plastic models can differ significantly from the flow stress to be adopted in a numerical analysis, also for perfectly plastic material modelling.

Hence, this study offers some guidelines in setting some validity limits for the perfectly plastic approach of solving structural impact problems.

Acknowledgements: The financial support of FAPESP, a research funding agency of São Paulo, Brazil through grants 97/14072-9 and 98/2856-8 is acknowledged. J. Yu wishes to express his gratitude to the support of the National Natural Science Foundation of China through project No.19672060.

References

[1] M. Alves. Material constitutive law for large strains and strain rates. *Journal Engineering Mechanics*, 126(2):215–218, 2000.

[2] M. Alves and N. Jones. Failure of beams using Damage Mechanics:Part I – Theory. *International Journal of Impact Engineering*, 27(8):837–861, 2002.

[3] D.J. Bammann, M.L. Chiesa, M.F. Horstemeyer, and L.I. Weingarten. Failure in ductile materials using finite element methods. In N. Jones and T. Wierzbicki, editors, *Structural Crashworthiness and Failure*, pages 1–54. Elsevier Science Publishers, Barking, Essex, 1993.

[4] Karlsson Hibbitt and Inc. Sorenson. *ABAQUS User's and Theory Manuals, VERSION 5.7*. H.K.S.& Inc., 1996.

[5] B.S. Holmes, S.W. Kirkpatrick, J.W. Simons, J.H. Giovanola, and L. Seaman. Modelling the process of failure in structures. In N. Jones and T. Wierzbicki, editors, *Structural Crashworthiness and Failure*, pages 55–93. Elsevier Science Publishers, Ltd., Barking, Essex, 1993.

[6] R. Huang and J. Yu. A simplified elastic-plastic model for dynamic responses of beams. In *Proceedings of the 2nd International Symposium on Impact Engineering, p. 95–100, Beijing, PRC*, 1996.

[7] W. Johnson. The elements of crashworthiness: scope and actuality. *Institution of Mechanical Engineers*, 204:255–273, 1990.

[8] N. Jones. *Structural Impact*. Cambridge University Press, 1989.

[9] N. Jones and T. Wierzbicki. *Structural Crashworthiness and Failure*. Elsevier Applied Science, Barking, Essex, 1993.

[10] D. Karagiozova and Marcílio Alves. Transition from progressive buckling to global bending of circular shells under axial impact. *International Journal of Solids and Structures (submited)*, 2003.

[11] F. Lu and A. N. Sherbourne. Shear-bending interactions for strain-hardening beams. *International Journal of Mechanical Sciences*, 34:789–804, 1992.

[12] M. A. Meyers. *Dynamic Behaviour of Materials*. John Wiley & Sons, Inc., NY, 1994.

[13] J.M. Mosqueira, P.S. Symonds, and H. Kolsky. On elastic–plastic and rigid–plastic dynamic response with strain rate sensitivity. *International Journal of Mechanical Sciences*, 27:741–749, 1985.

[14] USA National Research Council. *Committee on Tank Vessel Design, Tanker Spills: Prevention by Design*. National Academy of Sciences, USA, 1991.

[15] T. Nonaka. Some interaction effects in a problem of plastic beam dynamics. *Journal of Applied Mechanics*, 34:623–643, 1967.

[16] A. Paluszny. State-of-the-art review of automobile structural crashworthiness. *American Iron and Steel Institute*, 1992.

[17] N. Perrone and P. Bhadra. A simplified method to account for plastic rate sensitivity with large deformations. *Journal of Applied Mechanics*, 46:811–816, 1979.

[18] I. Planath, H. Norin, and S. Nilsson. Severe frontal collisions with partial overlap – significance, test methods and car design. *International Congress and Exposition, SAE Technical Paper Series*, pages 15–21, 1993.

[19] S. R. Reid and X. G. Gui. On the elastic-plastic deformation of cantilever beams subjected to tip impact. *International Journal of Impact Engineering*, 6:109–127, 1987.

[20] A. N. Sherbourne and F. Lu. Effect of axial restraints on the deflection of strain hardening beams. *International Journal of Mechanical Sciences*, 35:397–413, 1993.

[21] P. S. Symonds. Approximation techniques for impulsively loaded structures of rate sensitive plastic behavior. *SIAM Journal of Applied Mathematics*, 25:462–473, 1973.

[22] C. K. Youngdahl. Optimum approximate modes of strain-hardening beams. *International Journal of Impact Engineering*, 12:227–240, 1992.

[23] J. Yu and R. Huang. Numerical simulation and a simplified model for the early-stage response of a mild steel beam under impact loading. *Acta Mechanica Sinica*, 29(4):464–469, 1997.

[24] J. Yu and N. Jones. Numerical simulation of a clamped beam under impact loading. *Computers & Structures*, 32(2):281–293, 1989.

[25] J. Yu and N. Jones. Further experimental investigation on the failure of clamped beams under impact loads. *International Journal of Solids and Structures*, 27(9):1113–1137, 1991.

[26] J. Yu and N. Jones. Numerical simulation of impact loaded steel beams and the failure criteria. *International Journal of Solids and Structures*, 34(30):3977–4004, 1997.

[27] T. X. Yu. Elastic effects in the dynamic response of structures. In N. Jones and T. Wierzbicki, editors, *Structural Crashworthiness and Failure*, pages 109–127. Elsevier Science Publishers, Barking, Essex, 1993.